ISSN:1983 7402 ITA, 23 a 25 de setembro de 2014

RF Pulse Formation in NLTLs Using Varactor Diode

Lauro P. Silva Neto, José O. Rossi, Joaquim J. Barroso, Fernanda S. Yamasaki
Instituto Nacional de Pesquisas Espaciais, Av. Astronautas, 1758, São José dos Campos - SP

***Abstract* — Nonlinear transmission lines (NLTLs) have been investigated for high power RF generation in radars for military and civil applications in remote sensing and surveillance. The NLTL consists of an LC ladder network, where Cs and/or Ls are responsible for the nonlinearity. The objective of this paper is to study the behavior through a low power nonlinear capacitive line, using varactor diodes as nonlinear capacitors. Spice simulations are also used to investigate the behavior of NLTLs by varying some parameters in the NLTL circuit model such as number of sections, applied input pulse voltage amplitude and load. These simulations showed good agreement with the experimental results obtained from low voltage varactor diode line prototype built with 30 sections. Finally, the Fast Fourier Transform (FFT) spectrum of the signal extracted at the load was used to study the RF generation.**

***Keywords* — Soliton generation, RF pulse, nonlinear transmission line.**

I. INTRODUCTION

Nowadays research on communications for military forces are of primordial interest as interceptions of radio communication in battlefield in order to opt for attacking or defending. The radio communications is mostly used in civil and military applications as in airborne planes, satellites, ships military vehicles, etc. Radar is a system that employs radio waves or microwaves to determine the coordinates and speed of a target by using the reflection of electromagnetic waves [1]. Recently, the nonlinear transmission lines (NLTLs) have been investigated for producing the high power microwave signal to be used in radar applications. They could be used as pulse modular in a radar system as illustrated by the block diagram in Fig. 1.

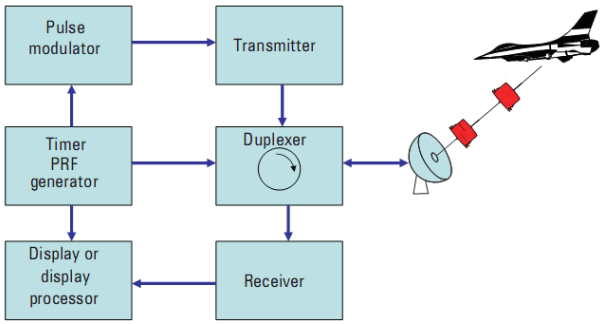

Fig. 1. Block diagram of a basic radar system [1].

The NLTLs use basically two components, capacitors and inductors, for RF production and at least one of these components need to be nonlinear, in which, respectively, the capacitance C(V) varies with voltage applied or inductance L(I) with the conduction current. Using ceramic capacitors as nonlinear medium in NLTLs according to [2], these lines have provided a signal of 60 MW peak power in the 100-200 MHz frequency range. On the other hand, as reported in [3], using ferrite-based inductors as nonlinear medium in NLTLs 20 MW peak power was produced at a frequency of the order of 1.0 GHz. A NLTL (consisting of nonlinear capacitors and/or inductors in cascade) produces output oscillations as follow. A square pulse injected into the line input is modified by the dispersive and nonlinear effects of the line, modulated and broken up into a group of solitons (oscillating pulses) which are used to feed an RF load through an antenna matched to the output of the line. In low-voltage NLTLs, varactor diodes are used as nonlinear medium since their diode junction capacitance varies with the inverse of the reverse voltage applied [4], [5]. In this work, the experimental results of a varactor diode NLTL built with 30 sections are presented. Besides, Spice simulation results are also used to compare with the experimental results obtained. Finally, the FFT of the simulated and experimental output voltage pulsed are used to investigate the frequency spectrum of the output oscillations obtained.

II. NLTL OPERATION THEORY

When an input pulse is injected into a dispersive LC line it propagates down the line length with a velocity given by $c = 1/(LC)^{1/2}$. If the line is nonlinear with variable capacitance C(V), the phase velocity is calculated by [6]:

$$V_p = 1/\sqrt{LC(V)}, \quad (1)$$

where C(V) is the variable capacitance per section as a function of the voltage applied, and L is the respective linear section inductance. The portion of the pulse with higher amplitudes will travel faster than its part with lower initial amplitude because the capacitance decreases with the pulse amplitude if ceramic capacitors or varactor diodes are used. In this way, the pulse peak catches up with the rising edge, forming an output shock wave front with a very fast rise time as shown in Fig. 2.

ISSN:1983 7402

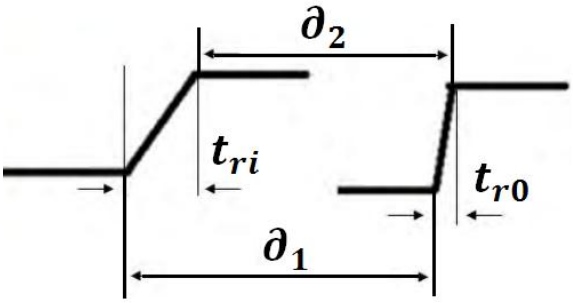

Fig. 2. Pulse rise time reduction in a NLTL.

A rough estimative for the pulse rise time reduction caused by the LC ladder sections is made by calculating the time delay difference between the lower amplitude portion and the peak of the propagation pulse as [6]:

$$\Delta T = t_{ri} - t_{ro} = \partial_1 - \partial_2 = n\left(\sqrt{LC_0} - \sqrt{LC(V_{max})}\right), \quad (2)$$

where:
- t_{ri} is the input rise time,
- t_{ro} is the output rise time,
- n is the number of sections of the line,
- C_0 is the unbiased capacitance,
- $C(V_{max})$ is the decreased capacitance at the maximum voltage applied,
- ∂_1 and ∂_2 are respectively the propagation delay times of the peak and lower amplitude portion of the input pulse, where $\partial_1 > \partial_2$.

A more accurate estimation is difficult because of the line nonlinearity. Then, the final rise time of the output compressed pulse (shock wave front) is calculated such as $t_{ro} = t_{ri} - \Delta T$, where $t_{ri} > \Delta T$.

On the other hand, if t_{ri} starts to decrease so that $t_{ri} \approx \Delta T$, t_{ro} cannot decrease to zero as the steepness of the output shock wave would become infinite. Therefore, the pulse-rise time reduction is limited ultimately by the cutoff frequency of the LC ladder (known as Bragg frequency) as the line is dispersive, which is

$$f_{co} = 1 / \pi \sqrt{LC(V_{max})} \quad (3).$$

As the propagating pulse cannot be submitted to further sharpening for a high number of sections because the energy cannot propagate above f_{co}, the spectrum of frequencies from the shock wave is separated, producing at the output a series of narrow pulses (solitary waves) with frequency close to the Bragg frequency depending on the value of the load.

Other important line parameter is its characteristic impedance given as follows [6]:

$$Z_0 = \sqrt{L/C(V)} \quad (4)$$

According to (4) the impedance of the line generally increases with the voltage applied because of the capacitance decrease when ceramic capacitors or varactor diodes are used as reported before.

III. Experimental Set-up and Simulation Modeling

The NLTL was made on a phenolite PCB using 30 sections with linear inductors of L = 2.7 µH and the BB809 varactor diode as nonlinear capacitors. Fig. 3 shows the experimental set-up with the PCB NLTL and the TTI pulse generator (model TGP 110), on the right side, responsible for producing the rectangular input pump pulse and, the digital Tektronix oscilloscope, on the left side, used to display and store the input and output signals. BNC connectors and 50 Ω coaxial cables were also used to make the connections between the PCB and oscilloscope/pulse generator devices.

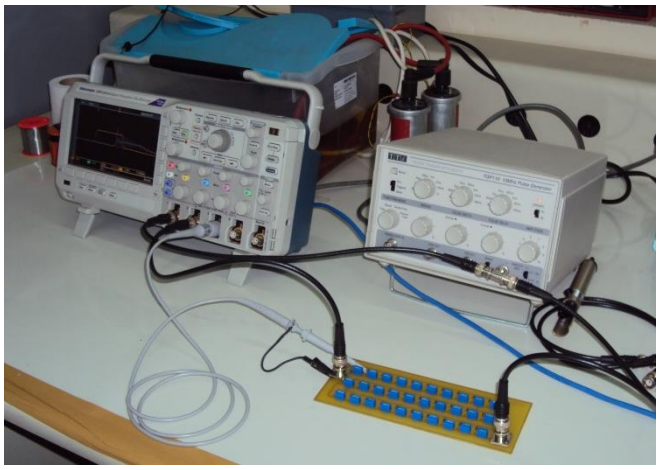

Fig. 3. Experimental set up for the NLTL tests.

The BB809 CxV curve obtained from manufacturer datasheet [7] is shown in Fig. 4. This curve can be modeled by a function given by [5]:

$$C(V) = C_{j0}/\left(1 + V/V_j\right)^m \quad (5)$$

where V_j is the diode junction potential, m is the nonlinearity factor and C_{j0} is the unbiased diode junction capacitance.

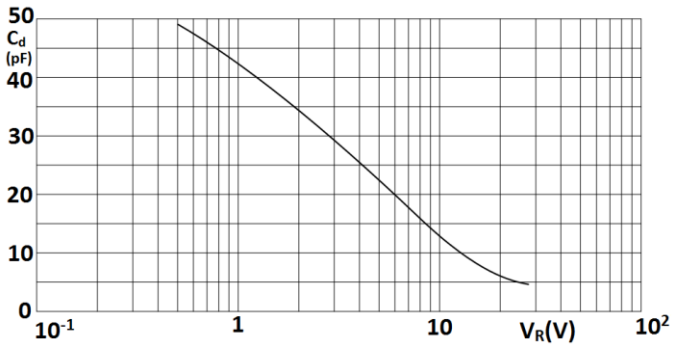

Fig. 4. Diode capacitance as function reverse applied voltage [7].

From the Fig. 4, by extrapolation one obtains that C_{j0} is of the order of 60 pF and $C(V_{max})$ of about 15 pF, which gives 75 % variation for the capacitance decrease at 9 V, which is the pulse amplitude used in the experiment for testing the

ISSN:1983 7402

NLTL. Other important parameters obtained from the datasheet are V_j= 0.7 V and m = 0.5.

For the simulation model, it was used the NLTL diagram circuit shown in Fig. 5, including ohmic losses of L and C (respectively, R_L = 0.56 Ω and R_C = 6.8 Ω) and the BB809 varactor diode with parameters discussed previously in last paragraph. The simulation was done by using 30 sections in Spice circuit model to compare with the corresponding experimental results.

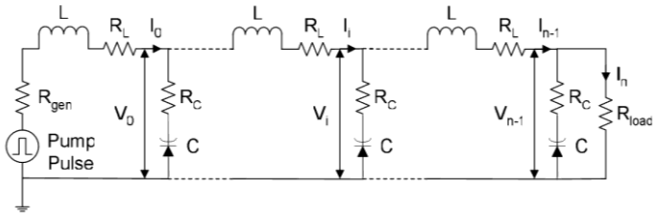

Fig. 5. NLTL schematic circuit used for NLTL simulation using BB809 varactor diodes.

IV. Results

A 50 Ω impedance pulse generator fed the line with a 9 V amplitude pump pulse of 310 ns duration and 15 ns pulse rise time. For maximum voltage amplitude of the pump pulse, the diode varactor gives C(V_{max}) of about 15 pF. Using (2) obtains ΔT = 190 ns, which certifies production of oscillations at the line output since t_{ri} << ΔT as discussed in section II. The experimental result confirmed that as shown in Fig. 6 by the voltage oscillations on section 29 for a load of 1 kΩ and a delay time measured of the order of 200 ns. In this case, the value of load resistance is not matched to the circuit because greater the mismatch, greater the amplitudes of the oscillations at the output. In fact, the NLTL is never fully matched to the load as the line characteristic impedance (see (4)) varies between the unbiased value of 212 Ω and that at the pulse peak of about 424 Ω. The frequency of the oscillations obtained is of about 40 MHz, which is close to the line cutoff frequency of the order of 50 MHz as expected.

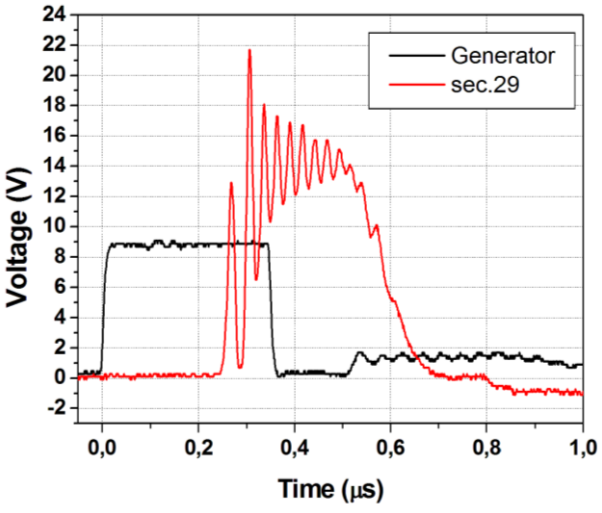

Fig. 6. NLTL experimental result for pulse voltage on section 29.

The NLTL Spice simulation obtained (shown in Fig. 7) for voltage on section 29 is also in good agreement with the experimental result of Fig. 6, which demonstrates the validity of varactor diode model used in the Spice simulator.

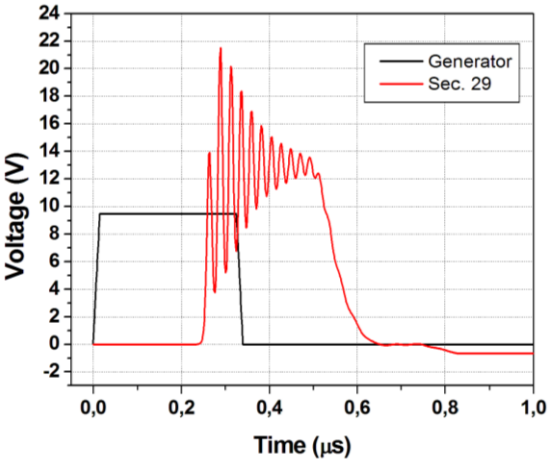

Fig. 7. NLTL simulation pulse voltage on section 29.

Fig. 8 illustrates the pulse propagation along the line showing the pulse voltages on different sections of the NLTL (sections 5, 10, 20 and 29). The increase in the pulse amplitude on section 29 is due to the reflected pulse caused by the load mismatch (1 kΩ) with positive reflection coefficient. However, the oscillation frequency in this case does not vary much along the line as we can note in the transient response of Fig. 8. Fig. 9 shows the corresponding simulation results obtained with a good accuracy compared to the experimental case given in Fig. 8. On the other hand, the Fig. 10 shows the effect of the load variation on the voltage modulation depth (VMD) and the output oscillation frequency generated on the output pulse on section 29. It is clearly that for a higher resistive load (1 kΩ) above the line matching impedance at full voltage (424 Ω), the oscillation frequency increases, but the VMD remains practically the same for all impedances. Also for lower loads, the DC level on the output pulse is reduced because of the negative voltage reflection at the load. Again, Fig. 11 shows the corresponding Spice simulation with a good fitting between both results.

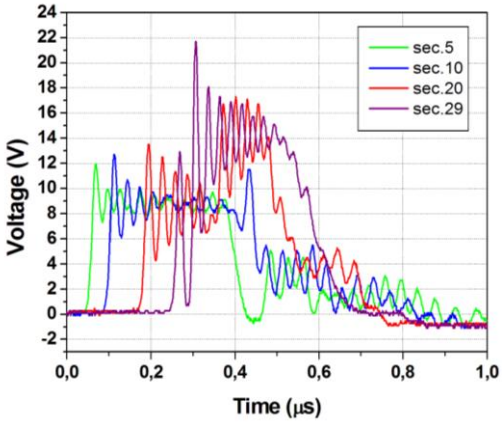

Fig. 8. Experimental voltage pulse obtained for the NLTL on different sections.

ISSN:1983 7402

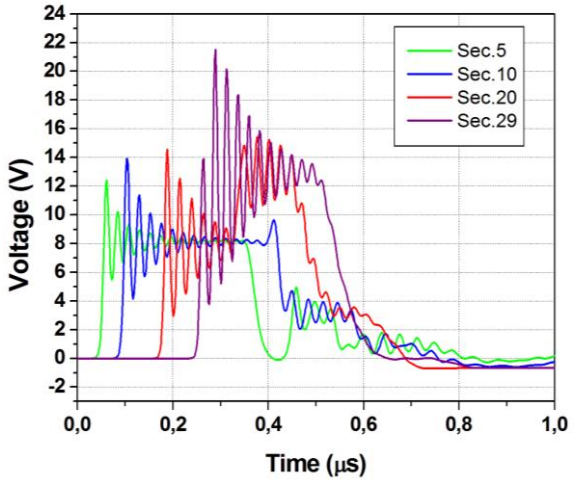

Fig. 9. Corresponding Spice simulation obtained for the NLTL on different sections.

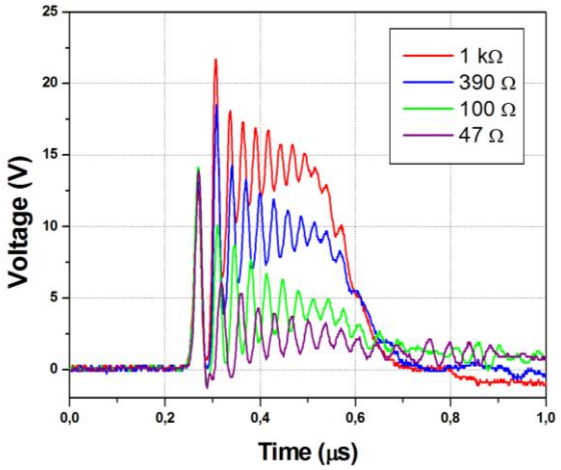

Fig. 10. Variation effect of load resistance on NLTL section 29.

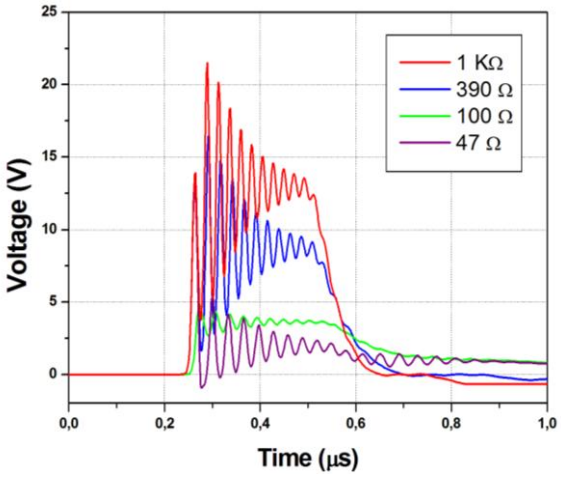

Fig. 11. Corresponding Spice simulation on NLTL section 29.

FFT spectra of the output voltage pulses given in Fig. 12 and 13 show more clearly the influence of the load on output oscillation obtained, which is in the range between f_{co} and $f_{co}/2$. As load is reduced the oscillation frequency tends to the half of the Bragg frequency (25 MHz) while in the opposite (load increase) the oscillation frequency tends to the Bragg frequency (50 MHz) as shown by the last lobes respectively in Figs. 12 & 13. The corresponding Spice FFT simulations for all loads is displayed in Fig. 14, where one can notice that the oscillation frequency increases with higher loads shown by the last lobes of the respective spectra.

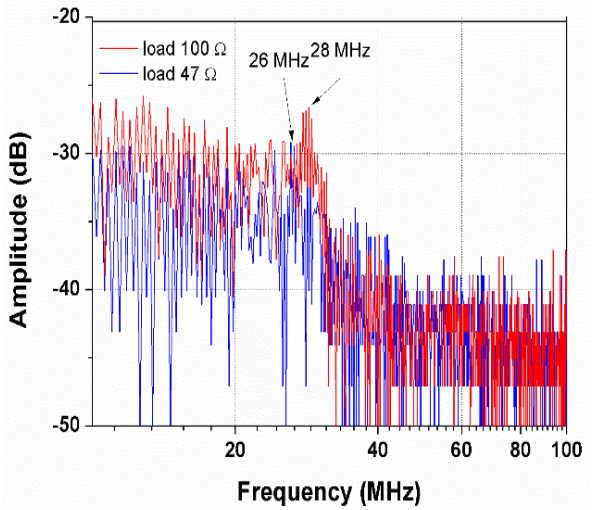

Fig. 12. FFT spectra of the NLTL output pulse with loads of 47 and 100 ohms.

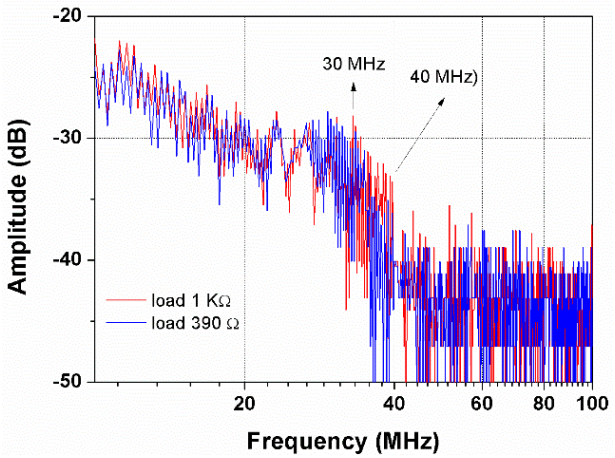

Fig. 13. FFT spectra of the NLTL output pulse with loads of 390 and 1 k ohms.

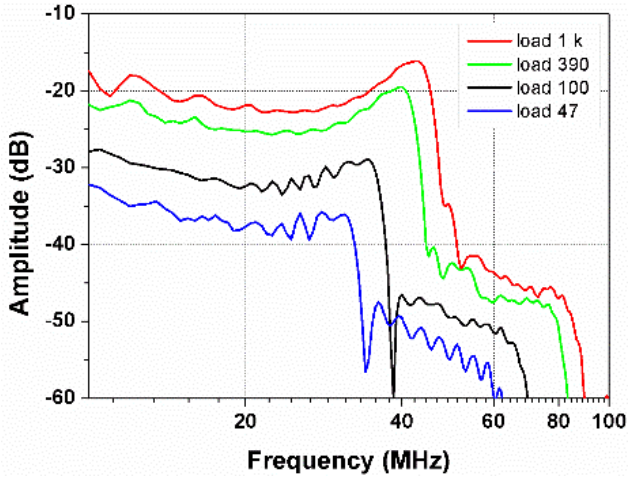

Fig. 14. Spice FFT spectra of the NLTL output pulse obtained for all loads.

ISSN:1983 7402

The experimental and simulation results of the output pulse on the 1.0 kΩ load varying the total number of sections of the PCB NLTL tested are shown in the Figs. 15 and 16, respectively, using the same parameters of the pump input pulse of previous tests. As shown the simulations are in a good agreement with the experimental results and the oscillation frequency remains practically the same around 40 MHz, not depending on the number of sections. For the experimental results with 30 sections, the oscillations of the output signal are more attenuated than that of the corresponding simulation due to the increase of the ohmic losses in longer lines in practice. Moreover, as n becomes larger the number and amplitudes of oscillations as well as the line delay time increase as shown in Figs. 15 and 16. However, for the case tested, optimum n lays between 20 and 30 as the number of oscillations are limited by the input pulse duration set at 300 ns.

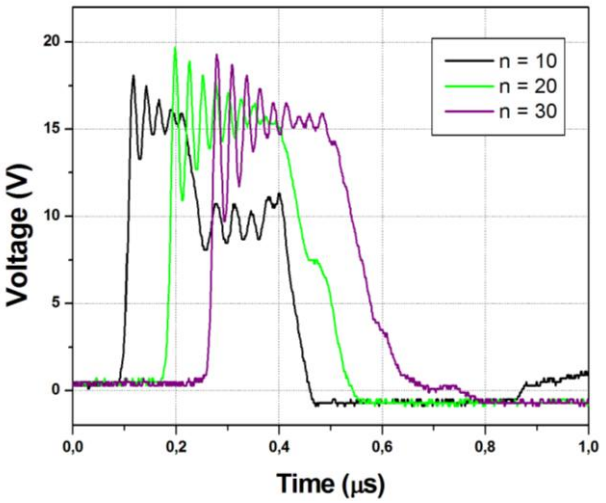

Fig. 15. Effect of the NLTL n increase on the output pulse on the load (last section).

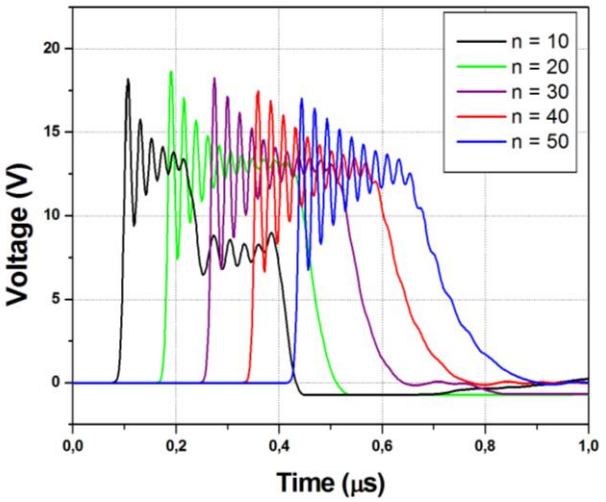

Fig. 16. Corresponding Spice simulation on the load with n increase up to 50.

The maximum voltage of generator, which reached only 12 V, limited the pulse amplitude applied of 10 V to the line input. The influence of the pump input pulse amplitude on the output oscillations was investigated for three different values (1 V, 5 V and 10 V) as shown by the NLTL output pulses in Fig. 17. We can see that low voltage amplitudes do not produce noticeable oscillations, as nonlinearity is too low to cause significant capacitance decrease. This experimental result also demonstrates that frequency tuning is achieved by controlling the pump pulse amplitude, as frequency of oscillations varies approximately between 30 and 40 MHz for a corresponding variation of amplitude in the range of 5-10 V. Spice simulations can produce similar results by varying the pump pulse amplitude in 5 V steps above 5 V (see Fig. 18). However, as seen in simulations, above 20 V distortion and attenuation on the output pulse oscillations start to degrade the system efficiency as amplitude approaches the diode reverse breakdown voltage of 30 V, with full attenuation at 25 V amplitude. Anyway, using higher pump pulse amplitudes up to certain value below the diode breakdown voltage is an excellent way to increase oscillation frequency. In Fig. 18, 15 V amplitude is the best case simulated for the generation of RF oscillations with lower attenuation and better VMD at 50 MHz approximately.

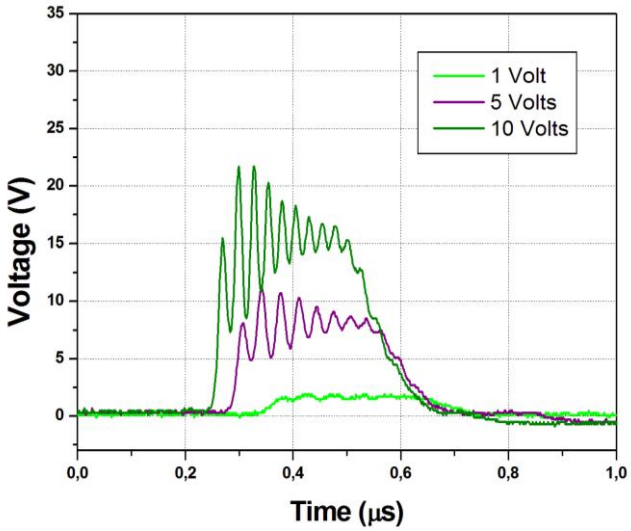

Fig. 17. Effect of the pump pulse amplitude on the output oscillations.

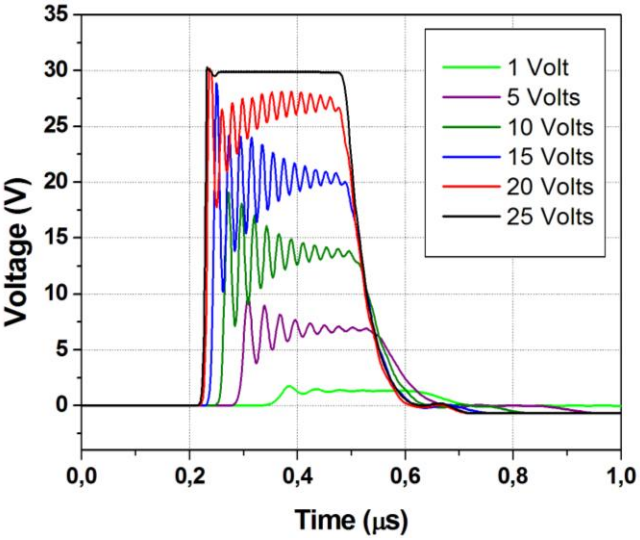

Fig. 18. Corresponding Spice simulations of the pump pulse amplitude effect on the output oscillations.

V. CONCLUSION

In this paper, it was shown that frequency and amplitude of the NLTL output signal are affected by key parameters such as number of sections, load and amplitude of the pump input pulse. The Spice model developed was validated by comparing Spice simulations with experimental results obtained with a low voltage NLTL prototype. The experimental and simulation results showed that the number of sections of the line does not change much the output oscillation frequency, but it has a strong effect on the number of cycles and amplitude of these oscillations. For the experimental case, the optimum number of sections appears to be n=30 using the pulse parameters of 10 V amplitude and duration of about 300 ns as the number of oscillations is larger with greater VMD and lower attenuation as shown in the Figs. 15 and 16. The oscillation frequency obtained in this case is around 40 MHz. Other important line parameter investigated was the value of the resistive load. It was observed that the voltage peak and the frequency of the oscillations increase as the load resistance becomes larger. The frequency of oscillations increases and approaches the line Bragg frequency in the limit. The 1 kΩ load was the optimum value found for producing soliton oscillations with frequency near 40 MHz as shown by the respective FFT the output pulse of Fig. 13. The amplitude of pump input pulse applied to the line also produces changes on the output pulse. It was demonstrated that oscillation frequency and cycle number increase with higher amplitudes of the pump input pulse. However, too large pulse amplitudes can lead to the output voltage saturation with suppression of oscillations because of the varactor breakdown voltage. Anyway, the optimum value of the input amplitude given by Spice simulations was 15 V with the higher number of cycles and lower attenuation of the voltage swing seen at 50 MHz.

ACKNOWLEDGMENT

The authors would like to thank the support funding provided by the Southern Office for Aerospace and Research Development (SOARD) from US Air Force under contract no. FA9550-13-1-0132.

REFERENCES

[1] Agilent Technologies Inc., “Agilent Radar Measurements”. Application Note, 2014, pp. 1-88.

[2] P. M. Brown and P. W. Smith, “High power, pulsed soliton generation at radio & microwave frequencies”, in Proc. of 11th International Pulsed Power Conf., 1997, pp. 346-354.

[3] B. Seddon, C. R. Spikings, and J. E. Dolan, “RF pulse formation in NLTLs”, in Proc. of 16th International Pulsed Power Conf., 2007, pp. 678-681.

[4] N. S. Kuek, A. C. Liew, E. Schamiloglu, J. O. Rossi, “Circuit modeling of nonlinear lumped element transmission lines including hybrid lines,” IEEE Transactions on Plasma Science, vol. 40, no. 10, pp. 2523-2534, Oct. 2012.

[5] F. S. Yamasaki, J. O. Rossi, J. J. Barroso, “RF generation using nonlinear transmission lines for aerospace applications,” In: SBMO/IEEE MTTS International Microwave and Optoelectronics Conference, Rio de Janeiro, 2013, pp. 1-5.

[6] P. W. Smith, “Transient electronics – pulsed circuit technology”, John Wiley & Sons, West Sussex, England, 2002, p. 245-249.

[7] Philips, “BB809 VHF variable capacitance diode,” Philips semiconductor, pp. 1-4, May 1996.